

## Identification of Binding Sites of EVI1 in Mammalian Cells\*

Received for publication, April 19, 2005  
Published, JBC Papers in Press, July 8, 2005, DOI 10.1074/jbc.M504293200

Bogdan Yatsula, Sharon Lin, Andrew J. Read, Amanda Poholek, Kristin Yates, Dongxian Yue, Pei Hui, and Archibald S. Perkins‡

From the Department of Pathology, Yale University School of Medicine, New Haven, Connecticut 06510

**The leukemia-associated protein EVI1 possesses seven zinc fingers within an N-terminal domain (amino acids 1–250) that binds to GACAAGATA. Single amino acid missense mutants of EVI1 were developed that failed to bind DNA either *in vitro*, as assessed by gel shift assay, or *in vivo*, as shown by transactivation studies. Specifically, mutation R205N lacks high affinity binding to the GACAAGATA motif. Putative EVI1 target genes were identified by using an EVI1-(1–250)-VP16 fusion protein that acts as a transcriptional activator with the binding specificity of EVI1. Sixteen genes induced in NIH 3T3 cells by wild type EVI1-VP16 but not by mutant forms were identified. Sequence analysis revealed evolutionarily conserved GACAAGATA-like motifs within 10 kb of their transcription start sites, and by chromatin immunoprecipitation in fibroblasts, we showed occupancy of many of these sites by EVI1-VP16. To assess whether native EVI1 binds to these sites in EVI1-transformed myeloid cells, we performed chromatin immunoprecipitation in 32Dcl3 and NFS58 cells, using anti-EVI1 antisera, and we showed that the majority of these sites is bound by wild type EVI1. These putative target genes include *Gadd45g*, *Gata2*, *Zfpm2/Fog2*, *Skil* (SnoN), *Klf5* (BTEB2), *Dcn*, and *Map3k14* (Nik). In this study we demonstrated for the first time that the N-terminal DNA binding domain of EVI1 has the capacity to bind to endogenous genes. We hypothesized that these genes play a critical role in EVI1-induced transformation.**

*Evi1* (for ecotropic viral integration site 1) is a complex locus on mouse chromosome 3 encoding a set of zinc finger protein isoforms. In retrovirally induced murine myeloid leukemias, proviral insertions at *Evi1* occur at two discrete sites at the 5' end of the *Evi1* locus, resulting in overexpression of the gene (1, 2). Chromosomal rearrangements involving the *EVI1* locus have been implicated in human myelodysplastic syndrome and myeloid leukemias (3–7). It is postulated that the resultant overexpression or dysregulation of the gene causes a block in terminal differentiation of myeloid cells (8, 9).<sup>1</sup> The mechanism by which this occurs is not known, although EVI1 has been shown to stimulate the cell cycle (11, 12). Unfortunately, no

bioassays for the leukemogenic effects of EVI1 have been reported. However, it has been shown to induce colony formation of Rat1 fibroblasts (13, 14).

*Evi1* encodes several protein isoforms as a result of alternative splicing (15–17) and alternative starts of transcription (18). The most well studied of these isoforms is a 135-kDa protein with 10 zinc finger motifs present in two different domains separated by 480 amino acids. DNA-protein binding analysis has revealed that EVI1 binds to specific DNA sequences, with the N-terminal domain binding to GACAAGATA-like sequences (19, 20) and the C-terminal domain binding to GAAGATGAG (21). Analysis by Delwel *et al.* (20) suggested that zinc fingers 4–7 are critical for the sequence-specific binding of the first set of zinc fingers. In an effort to identify genomic targets of the EVI1 protein, Kim *et al.* (22) used an *in vitro* selection for sequences that bound to EVI1 with high affinity and found that one of these is located within the *Itpr3* gene. The other EVI1-binding sites identified in this screen, however, were not situated near genes,<sup>2</sup> suggesting these sites are not linked to EVI1 target genes. To date, only one *bona fide* target gene of EVI1 has been reported (60).

The presence of zinc fingers capable of sequence-specific DNA binding suggests that EVI1 is a transcriptional regulatory protein. Transfection assays for transcriptional activation by EVI1 using synthetic reporters bearing EVI1-binding sites indicate that EVI1 can act as either a transcription repressor (8, 23, 24) or an activator (25, 26). A repression domain (comprised of amino acids 584–590, PLDLS) has been identified in EVI1 in a region N-terminal to the second zinc finger domain (24). Interaction between this domain and the CtBP family of transcriptional repressors (27) is critical for the ability of *Evi1* to promote growth of Rat1 fibroblasts in soft agar (28). Mutant forms of *Evi1* lacking the N-terminal (first) zinc finger domain act as dominant-negative alleles in this transformation assay, suggesting that sequestration of CtBP or other factors can block *Evi1* action (28).

We hypothesized that *Evi1* deregulation by retroviral insertion or chromosomal rearrangements in both murine and human leukemias likely leads to inappropriate deregulation of downstream target genes, and this is causally linked to leukemogenesis. This is supported by the finding that transformation of Rat1 fibroblasts requires the N-terminal zinc finger domain (13). The identification of EVI1 target genes will very likely shed light on the molecular etiology of EVI1-induced leukemias.

In this paper, we report the development of EVI1 mutants with single amino acid changes that are deficient in DNA binding via the first set of zinc fingers. In order to define which genes are modulated by EVI1, we have developed a system to rapidly activate and identify EVI1 target genes. Our approach utilizes an EVI1-VP16 transactivator fusion protein comprised

\* This work was supported by NCI National Institutes of Health (NIH) Grant RO1 81216 and Grant RPG-99-204-01 from the American Cancer Society. The costs of publication of this article were defrayed in part by the payment of page charges. This article must therefore be hereby marked "advertisement" in accordance with 18 U.S.C. Section 1734 solely to indicate this fact.

‡ To whom correspondence should be addressed: P. O. Box 208023, New Haven, CT 06520-8023. Tel.: 203-785-6843; Fax: 203-785-7467; E-mail: archibald.perkins@yale.edu.

<sup>1</sup> Y. Xiao, B. Yatsula, S. Lin, and A. Perkins, manuscript in preparation.

<sup>2</sup> A. S. Perkins, unpublished data.

TABLE I  
Mutagenic oligonucleotides

Mutation	Sequence
Q199D	GCC ATA AAT CCT ATA CTG ACT TTT CAA ACC TTT GTC G
Q199D antisense	CGA CAA AGG TTT GAA AAG TCA GTA TAG GAT TTA TGG C
R205N	GTT TTC AAA CCT TTG TAA TCA TAA GCG CAT GCA TGC
R205N antisense	GCA TGC ATG CGC TTA TGA TTA CAA AGG TTT GAA AAC
R205K	GTT TTC AAA CCT TTG TAA ACA TAA GCG CAT GCA TGC
R205K antisense	GCA TGC ATG CGC TTA TGT TTA CAA AGG TTT GAA AAC
R205Q	GTT TTC AAA CCT TTG TCA GCA TAA GCG CAT GCA TGC
R205Q antisense	GCA TGC ATG CGC TTA TGC TGA CAA AGG TTT GAA AAC

of the first seven zinc fingers of EVI1 fused to the potent transcriptional activator VP16 and expressed under control of the tetracycline (tet)<sup>3</sup>-regulated system in cultured cells (29, 30). This chimera has the DNA binding specificity of EVI1 and is a strong activator of transcription via its VP16 domain. Up-regulated mRNA transcripts were identified by hybridization of labeled cDNA to oligonucleotide microarrays. Chromatin immunoprecipitation experiments demonstrate binding by EVI1-VP16 to GACAAGATA-like motifs located in *cis* to the regulated genes. These experiments reveal an interesting set of genes as potential targets for EVI1 regulation, which may help to explain EVI1-induced myeloid transformation.

## EXPERIMENTAL PROCEDURES

**Plasmid Constructs**—We derived *pHP-3*, a plasmid that places a chimeric EVI1-VP16 protein under the control of the tet operon within plasmid pUHD10-3 (29), as described previously (22). This chimera contains the first zinc finger domain of EVI1 (zinc fingers 1–7; amino acids 1–250) linked to the transcriptional activation domain of the herpes simplex virus VP16 protein.

To create mutations in zinc finger six, site-directed mutagenesis was performed by using a Stratagene Quik-Change kit. The mutagenic oligonucleotides are listed in Table I.

To create the hemagglutinin epitope-tagged version of EVI1, the 4.5-kb EcoRI fragment of plasmid p58.2-1 (1) encompassing the *Evi1* cDNA was inserted into the EcoRI site of pEFneo (31), as modified by S. Orkin; the HindIII-XbaI fragment containing the EF1 $\alpha$  promoter was moved to pBluescript KS, and a HindIII-NotI fragment was then moved to a plasmid containing a poly(A) site from SV40 with a NotI site at the 5' end and a SacI site at the 3' end. PGK-neo was then placed at the SalI site. A hemagglutinin tag was added to the C terminus of Evi1 by amplifying bp 3467–3603 with oligonucleotides 5'-CACAGGCATATGCTATGATG-3' and 5'-GGCCGCTTAGAGGCTAGCGTAATCCGGAA-CATCGTATGGGTATACATGGCTTATGGACTGGAT-3', digesting with NotI and NdeI, and inserting this into NdeI-NotI-digested pEFneo-Evi1. Evi1HA was transferred into the EcoRV site of pBluescript as a blunt-ended 3.6-kb EcoRI-NotI fragment. The downstream ClaI site was converted to BamHI, and Evi1HA was then transferred as a BamHI fragment to pBluescript KS+ to create pBS-Evi1HA(Bam), in which the T3 promoter lies upstream of the gene. This was transferred into pUHD10-3 as an EcoRI-XbaI fragment to create plasmid 718.

**Protein Purification**—Amino acids 1–250 of EVI1 were expressed in *Escherichia coli* strain DH5 $\alpha$  as a fusion protein with *Schistosoma trypanosoma* glutathione S-transferase using the pGEX-1N vector (Amersham Biosciences) following purification on glutathione affinity resin (Amersham Biosciences). Bacteria were grown in 0.4 liters of rich broth (25 g/liter bactotryptone, 10 g/liter yeast extract, 5 g/liter NaCl) at 37 °C to  $A_{600} = 0.6$ – $0.8$ , at which point IPTG was added to 0.5 mM. Following an additional 3 h of growth, cells were harvested, resuspended in 30 ml of PBS (137 mM NaCl, 2.68 mM KCl, 10 mM Na<sub>2</sub>HPO<sub>4</sub>, and 1.76 mM KH<sub>2</sub>PO<sub>4</sub>) containing 150 mM dithiothreitol, and protease inhibitors (2 mM phenylmethylsulfonyl fluoride (Sigma) and 2.3 mM disofoflorophosphate (Sigma); one Complete Protease Inhibitor Mixture tablet, EDTA-free (Roche Applied Science; catalog number 11330800) per 50 ml), and

lysed by three passes through a EmulsiFlex-C3 high pressure homogenizer (Avestin) at 15,000–20,000 p.s.i. Following clarification at 20,000 rpm for 15 min at 4 °C in an SS34 rotor, cells were rotated for 2 h at 4 °C in a 50-ml conical tube with 0.25 ml of glutathione-Sepharose 4B bead slurry and washed in PBS. The beads were collected by centrifugation at 2000 rpm for 5 min at 4 °C, discarding the supernatant. Following a wash with 5 ml of PBS, the beads were transferred to a microcentrifuge tube, where sequential 1-ml elutions were performed with 1.25 mM glutathione, 5 mM glutathione, and three elutions with 10 mM glutathione. Coomassie Blue-stained SDS-PAGE revealed that the third 10 mM glutathione elution was the most pure; earlier fractions were found to consist of a more heterogeneous array of proteins. Protein samples were assayed directly for gel shift activity. Protein concentrations were determined with the Bradford assay.

**Measurement of Protein-DNA Affinity**—The DNA binding activity of EVI1-GST proteins was assessed by electromobility shift assay on 4% polyacrylamide gels (40:1 acrylamide/bisacrylamide) containing 2.5% glycerol and buffered with 0.5 $\times$  TBE. Gels were run at room temperature at 35 mA. Preliminary experiments were performed to optimize the gel shift conditions. The probe DNA in these experiments was annealed (5'-TGTACTGACAAGATAACAGC-3' and 5'-AGCTGTATCTTGT-CAGTAC-3'), radiolabeled with [ $\gamma$ -<sup>32</sup>P]ATP (7000 Ci/mmol; ICN) and polynucleotide kinase (New England Biolabs) in a 20- $\mu$ l reaction composed of the manufacturer's buffer (10 pmol of DNA, 83  $\mu$ Ci of [ $\gamma$ -<sup>32</sup>P]ATP (12 pmol), and 10 units of enzyme), and purified by fractionation on a 5-ml G-50 column equilibrated with 10 mM Tris, pH 8.0, 50 mM NaCl, and 1 mM EDTA. The resultant probe had specific activity of 6,000 cpm/fmol of DNA. DNA binding reactions (20  $\mu$ l), consisting of 12.5% glycerol, 50  $\mu$ g/ml poly(dI-dC) (Amersham Biosciences), 5 mM MgCl<sub>2</sub>, 100  $\mu$ g/ml bovine serum albumin, 10 mM dithiothreitol, 50 mM HEPES, pH 7.9, 10  $\mu$ M ZnSO<sub>4</sub>, 50 mM NaCl, and protein were assembled on ice, incubated at 22 °C for 30 min, and then electrophoresed. The amount of protein and probe DNA in each reaction varied, as described under "Results." Dried gels were imaged and quantitated using a PhosphorImager (Amersham Biosciences). Numerical data of bound and free probe was the "sum minus background" from the ImageQuant software.

The  $K_{eq}$  determination for protein-DNA interactions was done using the approach described by Chodosh *et al.* (32). It is assumed that the stoichiometry of protein/DNA binding is 1:1 and that the binding reaction can be represented by  $D + P \leftrightarrow DP$ , where D is free DNA; P is free protein, and DP is DNA-protein complex. Under conditions of DNA excess, then  $[DP] = [P_T] \times ((K_{eq}[D_T]) / (1 + K_{eq}[D_T]))$ , where  $[D_T]$  and  $[P_T]$  are the total DNA and protein concentrations, respectively. Thus, the slope of the plot of  $[DP]$  against  $[P_T]$  can be used to derive  $K_{eq}$  (32). To calculate  $[P_T]$  for the wild type EVI1-(1–250)-GST, we saturated the protein with DNA and measured the amount of DNA-protein complex, which is equal to the amount of active protein. Because the mutant proteins were prepared in an identical manner, and because their level of purity was almost exactly the same, it was assumed that the moles of active protein per mass of total protein (determined by Bradford assay) was the same for the mutants as for wild type EVI1-(1–250)-GST protein. Based on this, 90 ng (determined by Bradford) of wild type EVI1-(1–250)-GST was found to contain 200 fmol of active protein, and by using this relationship between total protein and active protein, the molar concentrations for the other preparations were defined. Proteins were serially diluted with 1 $\times$  binding buffer, and 10–50 fmol were used in binding reactions with 1250 fmol of DNA. Quantitation of fmol of DNA bound was performed by EMSA and Phosphorimager as described above, and through analysis of these binding data, the  $K_{eq}$  was determined.

**Cell Lines and Related Techniques**—NIH 3T3 cells expressing the autoregulatory tet repressor-VP16 chimera, pTet-tTAK (designated as S2-6 cells), were generously provided by D. G. Schatz (30). S2-6 cells were maintained in histidine-deficient Dulbecco's modified Eagle's

<sup>3</sup> The abbreviations used are: tet, tetracycline; CAT, chloramphenicol acetyltransferase; ChIP, chromatin immunoprecipitation; IPTG, isopropyl 1-thio- $\beta$ -D-galactopyranoside; PBS, phosphate-buffered saline; DME, Dulbecco's modified Eagle's; TGF, transforming growth factor; GST, glutathione S-transferase; EMSA, electrophoretic mobility shift assay; TK, thymidine kinase; TSS, transcription start site; HA, hemagglutinin.

TABLE II  
Primers for quantitative reverse transcription-PCR

Gene	Forward (5'-3')	Reverse (5'-3')
<i>Gadd45g</i>	AACGACATTGATATCGTGCGCG	TCACCAAGTCGATCAGACCAAG
<i>Gata2</i>	CAAGATGAATGGACAGAACC GG	TGGATTTGCTGGACATCTTCCG
<i>Gata3</i>	CTTATCAAGCCCAAGCGAAG	GCTAGACATCTTCCGGTTTC
<i>Evi1</i>	TGGAGATGAGCTGTAAGG	GGAACTCCTTGTCAGACAGTGAC
<i>Klf5</i>	TACAACAGAAGGAGTAACCCGG	TGCGGTTTAAAGGATGGCAGAG
<i>Map3k14</i>	ATCCAGTCTCTCAATGGCGAAC	CGAGCACTGAGATCAAAGGAAG
<i>Napb</i>	GCTCATGAGGAACAGAACAGTG	ACATGACACAGACATGGTGAGC
<i>Skil</i>	TACAGAGTGAGCATGCTCAGAG	CTGCAGCTTCAGCTCCTTTATC
<i>Tnnt2</i>	TATTCACAACCTGGAGGCTGA	AAACAGGAGTCTGCATTGGGTG
<i>Zfpm2</i>	CTGGGGTAGAGACAGATGACTG	ACAAAGGCGACGAGCTTTCAC

(DME, Irvine Scientific Inc.), containing L-histidinol (0.5  $\mu$ M) and tet (0.5  $\mu$ g/ml) at 37 °C, 5% CO<sub>2</sub>. Stable S2-6 cells containing the tet-responsive wild type (pHP3) or mutant (pHP3<sup>R205N</sup>) *EVI1-VP16* fusion gene or containing the wild type 135-kDa EVI1 (plasmid 718) were generated by cotransfection of S2-6 cells with one of the plasmids plus pBABE-puro (33) by calcium phosphate or with FuGENE transfection reagent (Roche Applied Science) followed by puromycin selection as described (22). Single cell-derived colonies were expanded in medium containing puromycin (2  $\mu$ g/ml) and tet (0.5  $\mu$ g/ml) to obtain individual clonal cell lines. Clones were screened for induction by Western blot (see below). Table IV shows the cell lines used in this study. For induction of EVI1-VP16, cells were washed twice with PBS and then cultured in histidine-deficient DME medium without tet for 15 h. Assays for transactivation of the chloramphenicol acetyltransferase (CAT) reporter were conducted as described (22).

NFS58, 32Dcl3, DA-1, NFS-58, NFS-60, NFS-78, and FDCP-GM cells were cultured in DME medium supplemented with fetal bovine serum (10%), conditioned medium from WEHI cells (10%; a source of interleukin-3), penicillin, streptomycin, and glutamate.

**Generation of Anti-EVI1 Antiserum**—For N terminus-specific antiserum, rabbits were immunized with purified protein comprising amino acids Met<sup>1</sup>–Gly<sup>249</sup> of murine EVI1 (based on GenBank™ accession number M21829). Soluble protein was used to serially immunize a rabbit, and bleeds were tested by enzyme-linked immunosorbent assay. The N-terminal polypeptide was produced in *E. coli* strain BL21(DE3) as a hexahistidine-tagged entity and was purified by affinity chromatography on a nickel resin (Novagen) essentially as described (34). The expression construct for the N-terminal peptide was generated by PCR amplification by using forward primer 5'-CTTGCTGCATATGAA-GAGTGAAGAGGACC-3', containing an NdeI site, and reverse primer 5'-GGCCCTCGAGTCCACTGCCGCAAAATGG-3', containing an XhoI site. The PCR product was cut with NdeI and XhoI and inserted into expression vector pET22b(+), cut with XhoI and NdeI, and transformed into BL21(DE3). To produce protein, bacterial cells containing recombinant expression vector were grown in Luria-Bertani broth with 100  $\mu$ g/ml ampicillin. At A<sub>600</sub> = 0.7, cells were induced with 0.5 mM IPTG and grown for an additional 3 h. Cells were harvested and lysed in 25 mM Tris, pH 8.0, 30 mM imidazole, 0.5 M NaCl by sonication. The clarified extract was applied to a 4-ml Ni<sup>2+</sup> resin (Novagen) and washed with 10 column volumes each of 30 mM imidazole, 0.5 M NaCl, and 50 mM imidazole, 0.1 M NaCl. Proteins were eluted with 0.2 M imidazole, 0.1 M NaCl, pH 8.0. The eluant (30 ml) was concentrated to 3 ml using a Fisher Concentrator 10K, spun at 2,000 rpm for 3 days, and then dialyzed against phosphate-buffered saline containing 10 mM imidazole. After removing insoluble protein, the concentration was adjusted to 0.4 mg/ml protein and 0.1% SDS and then boiled for 8 min prior to injection into a single rabbit, as a series of five injections over several months. To generate C terminus-specific antiserum, a rabbit was immunized with a fragment of EVI1 comprising Lys<sup>719</sup>–Pro<sup>734</sup> and Asn<sup>805</sup>–Val<sup>1042</sup>. The immunogen was purified from *E. coli* expressing plasmid as a hexahistidine-tagged protein as described above. Expression constructs were created in pET22b(+), by inserting a PCR product generated from an EVI1 cDNA containing a deletion of amino acids Arg<sup>735</sup>–Glu<sup>804</sup>, created by second strand synthesis of a uracil-substituted single-stranded template using oligonucleotide (5'-CAGACATGTTGC-CGTTCCGAAATATCTTGCCAC-3'). PCR amplification was done with a forward primer containing BamHI site and sequence 5'-CGGAAC-CCCAAAGAGCGCTACACC-3' and a reverse primer containing XhoI site and sequence 5'-TACATGGCTTATGGACTGGATGGC-3'. PCR products were cut with BamHI and XhoI, inserted into similarly cut pET22b(+), and introduced into BL21(DE3). A 1-liter culture was induced with 0.5 mM IPTG, grown for 3 h, harvested, solubilized in 5 M guanidine, and loaded onto a 5-ml nickel resin column (Novagen),

washed (10 column volumes) with 2 M guanidine, 20 mM imidazole, washed (10 column volumes) with 0 M guanidine, 50 mM imidazole, and then eluted with 200 mM imidazole, 0.1 M NaCl. To peak fractions, SDS was added to 0.1%, and the sample was boiled for 3 min. The sample was then diluted 1:1 with PBS + 0.1% SDS, concentrated, and then diluted and concentrated again. The preparation (0.4 mg/ml) was filtered and used for injection of one rabbit.

**Immunoprecipitation and Western Blot Analysis**—For immunoprecipitation, cells were lysed, and lysates were immunoprecipitated with 5  $\mu$ l of antiserum per 0.5 ml of cell lysate, as described previously (35). For Western blots, induced cells (16 h after removal of tetracycline) or uninduced cells were washed with PBS, lysed in SDS-PAGE loading buffer (200  $\mu$ l/60-mm dish), boiled for 10 min, and clarified by centrifugation (8 min, full speed, Eppendorf microfuge). Protein extracts were fractionated on 10% acrylamide SDS-polyacrylamide gels. Proteins were electroblotted onto nitrocellulose membranes. Blots were probed with anti-EVI1 antiserum specific for the N terminus, followed by secondary anti-rabbit horseradish peroxidase, and development of chemiluminescence with Pierce reagent.

**Microarray Analysis**—Total RNA was isolated from induced cells by guanidinium thiocyanate/phenol chloroform extraction (36) (Trizol; Invitrogen). 50  $\mu$ g of total RNA was reverse-transcribed with oligo(dT) primer and murine leukemia virus reverse transcriptase (SuperscriptII) substituting allyl amine dUTP (Sigma) for 60% of the dTTP. Following hydrolysis of the RNA and cleanup, the cDNA was labeled using monoreactive Cy3 and Cy5 (Amersham Biosciences) at room temperature for 30 min, followed by quenching of the reaction with hydroxylamine, and purification of the labeled cDNA by Microcon YM30 spin columns. OMM13.4K oligonucleotide arrays were generated at and purchased from the Keck DNA Array Facility ([info.med.yale.edu/wmkeck/dna\\_arrays.htm](http://info.med.yale.edu/wmkeck/dna_arrays.htm)) and contained 13,400 70-mer single-stranded oligonucleotides for mouse genes. Slides were hybridized for 30 h at 42 °C in 30% formamide, then washed with sequential buffers (2 $\times$  SSC, 1 $\times$  SSC, etc., 15 min each at room temperature with agitation), and then scanned on an Axon scanner at 532 and 635 nm.

**Data Analysis**—Replicate hybridizations were normalized by linear regression scaling, and then up-regulated genes were identified using fold induction and Student's *t* test criteria. Genes with low signal intensity (less than 25 pixels) were rejected. These analyses were performed using software available on the Yale microarray data base ([ymd.med.yale.edu/ymd\\_prod/cgi-bin/gz\\_login.cgi](http://ymd.med.yale.edu/ymd_prod/cgi-bin/gz_login.cgi)) and Microsoft Excel.

**Quantitative Real Time PCR**—Quantitation of relative mRNA abundance for specific up-regulated genes was performed by real time PCR amplification of cDNA prepared from total RNA by reverse transcription with an oligo(dT) primer and modified Moloney murine leukemia virus reverse transcriptase (SuperscriptII; Invitrogen). Reactions were performed in the presence of SybrGreen as supplied (Invitrogen) on a thermal cycler equipped with excitation and detection capabilities (i-Cycler, Bio-Rad) and that provided threshold cycle (*C<sub>T</sub>*; determined at the end of the extension step) values as numerical output. To create a reference curve to convert *C<sub>T</sub>* value to relative mRNA amount, *C<sub>T</sub>* values for a particular gene were determined (in triplicate) for three serial dilutions of one sample, and the log of relative volume was plotted against the *C<sub>T</sub>* value, and an equation was derived. By using this equation, the *C<sub>T</sub>* value of unknown samples was related to the "standard" sample. For each sample,  $\beta$ -actin was repeated to quantitate a correction value, which was used to normalize data. The quality of all PCR products was confirmed by melt-curve and ethidium bromide-stained agarose gel analysis.

**Chromatin Immunoprecipitation (ChIP)**—ChIP analysis was performed essentially as described (37). Immunoprecipitations were performed with the rabbit polyclonal antiserum specific for the N- and C-terminal regions of EVI1, produced as described above. Primers for PCR amplification of immunoprecipitated DNA are shown in Tables II and III.

TABLE III  
Primers for chromatin immunoprecipitation

Gene	Binding site	Relative position	Forward	Reverse	Length
<i>AP17</i>	GACAAGATA	-109	GTGTGAAAACGACGCCAGT	TTCGAATTCGCCAATGACAAGACGC	200
<i>Dcn</i>	AGAAGATAA	4700	ATTCCCTGCATTCTCTGGTCTG	TGGGCCTCCAACTTCTGAAG	200
<i>Drd1ip</i>	ACAAAATAA	-7993	ATCCAGGGATCAGTTGGATTGC	GTCCTCAGCTCTCTAAAAGGCTTG	287
<i>Gadd45g +2500</i>	TTATCTTTT	2543	GTCACAGCCGTGATGGAAGTTA	AGCCAGAAGCACTAAGCTACAG	233
<i>Gata2 -3000</i>	AGATAAGAAAC	-2880	GACTTTATCAGCCTGCCCATCG	CTCGGCCGGCTAATCTTTGTTC	258
<i>Gata3</i>	GACAAGATA	-7200	TTCTACCTTTGCTGTGAAGCC	ATGCAGTAAACTGAGGAGAG	261
<i>Klf5 -3100</i>	GTATCTTCTCT	-3141	GATACGAAGTGTCTACGGGAC	ACCTCTGGTCAGTTGAACACAG	235
<i>Map3k14</i>	TCATCTTGT	-2666	TCAGTTTGTGGAGTCTGTGTCG	TGAGCAAGAGAGCTGTACCATC	217
<i>Napb</i>	AGATAAGATAT	-8829	GACTCTTGAATTGCATGGGCAC	CCAGGCTCTTTGCTCTACATAC	215
<i>Plagl1</i>	TTATCTTGTG	1771	AACGGTCTACTCAGAAGCTAGC	GGTTACAATGAGGAGGGAAGC	215
<i>Skil +1400</i>	TGACAAGAGAA	1425	CAATGTCAGGGTCTCTTTGCC	ATGAACAAGCCGAAGCACTAGC	352
<i>Skil +5400</i>	TATCTTCTCTG	5386	TTTCAGTTCATGCTTCTCTCC	AAGGCCTTGATTTGACCTCAG	195
<i>Tnnt2</i>	AGAAAAGATAA	5762	TCTCTTTTGCCTGACCTTCTC	AGATGGAACCTAGCCAGGTTGC	251
<i>Zfpm2 -2500</i>	CACAAAATAA	-2509	GAAGGGAGCTATTTCATTTTCAG	CCCTATAAGCAATTATCTCTGTCC	435
<i>Zfpm2 -3200</i>	GATAAAATACAAGATAT	-3229	GTACCTTCTACCTTTCCTCC	GCTCCACACACTGTTTGGTAC	324

## RESULTS

*Amino Acids Gln<sup>199</sup> and Arg<sup>205</sup> Are Critical for Sequence-specific DNA Binding in Vitro*—Previous studies by Delwel *et al.* (20) indicated that zinc fingers 4–7 of EVI1 were necessary for EVI1 to bind to DNA with sequence specificity. From structural studies of zinc finger motifs, it is known that the C-terminal side is comprised of an  $\alpha$ -helix that is held in place by an internal hydrophobic core mediated by the interaction of the side chains of the conserved phenylalanine residue and the leucine residue (also invariant) located in the central portion of the  $\alpha$ -helix (Fig. 1a). The amino acid side chains that interact with DNA are situated on the outer face of the  $\alpha$ -helical region, specifically those located at positions 2, 3, and 6 of the helix, but also include the amino acid at position -1 relative to the helix (38). A “recognition code” has been put forth for the correspondence between amino acids at positions -1, 3, and 6 and specific bases in the DNA (39). Typically, one finger recognizes a three-base “subsite” within a larger recognition motif that requires the concerted binding of multiple zinc fingers. Inspection of the amino acid sequence of EVI1 reveals that zinc finger six possesses amino acids at -1 (Gln), 3 (Asn), and 6 (Arg) that are favorable for DNA binding (Fig. 1b). To test their possible involvement in sequence-specific binding, we created mutations at two of these sites within GST fusion proteins containing amino acids 1–250 that compose the N-terminal zinc finger region. These proteins were purified (Fig. 1c), and their affinity for binding to the GACAAGATA motif was determined by quantitative equilibrium binding measurements using electromobility shift assay to assess DNA binding. First, the active component of wild type EVI1-(1–250)-GST was determined as described by Riggs *et al.* (40) by saturating the protein with DNA and quantitating the amount of DNA bound under conditions of vast DNA excess (data not shown). The proteins were then titrated against a fixed amount of DNA, and the quantity of protein-DNA complex was determined (Fig. 1d). By plotting the input protein concentration against the concentration of protein-DNA complexes present on EMSA (Fig. 1e) and calculating the slope, the affinity was determined by using standard equilibrium binding equations (32). Although the wild type protein had a binding affinity over  $10^9 \text{ M}^{-1}$ , each of the mutants was compromised in their DNA binding ability as follows: R205N and R205Q had no detectable binding ability, whereas Q199D retained some, albeit very weak, affinity for DNA (Fig. 1f). The R205K mutation, the most conservative of the changes, retained the highest activity, but still this was only slightly better than 1/200th of wild type affinity (Fig. 1f).

*Amino Acid Arg<sup>205</sup> Is Critical for Sequence-specific DNA Binding in Vivo*—From these studies, it is apparent that the R205N mutant is unable to bind *in vitro* to the GACAAGATA

motif with significant affinity. With the goal of using this mutant within mammalian cells, we then sought to determine whether the R205N mutant protein was also incapable of sequence-specific DNA binding *in vivo*. To assess this, we assayed the activation of a pTK-CAT reporter plasmid harboring five copies of the GACAAGATA-binding motif upstream of the minimal TK promoter region (plasmid pAP17; Fig. 2c). Because EVI1 is a repressor and is unable to activate such reporters (23), we used chimeric EVI1-VP16 constructs comprised of the zinc finger region (amino acids 1–250) fused to the potent transcriptional activation domain of the herpes simplex virus VP16 protein (Fig. 2a). We have shown previously that such a chimera containing wild type EVI1 N-terminal zinc finger region is able to activate transcription of a reporter plasmid containing the GACAAGATA motif (23). We created an analogous EVI1<sup>R205N</sup>-VP16 chimera, placed both wild type and mutant constructs under control of the tetracycline operons (29), and transferred these constructs into S2-6 cells, an NIH 3T3 derivative harboring an autoregulatory tetracycline-regulated expression system (30). Single cell-derived cell lines harboring EVI1<sup>R205N</sup>-VP16 were established and were tested for the tet-regulated induction of the EVI1-VP16 chimera by Western blot. Line R205N13 (referred to as RN13; Table IV) was found to express EVI1<sup>R205N</sup>-VP16 protein upon removal of tetracycline (Fig. 2b, lane 3). We have reported previously the creation of a similar cell line, termed 6D (Table IV), in which EVI1-VP16 is regulated in a similar manner (22) (Fig. 2b, lane 1). The cell lines used in these studies are tabulated in Table IV.

To test if these EVI1-VP16 chimeras could bind the GACAAGATA motif *in vivo*, we grew the RN13, 6D, and parental S2-6 cells in the absence of tetracycline to induce the tet promoter, and we transfected the cells with either pTK-CAT or pAP17. Assay of CAT activity in these cells revealed significant reporter activity only in 6D cells, expressing the wild type EVI1-VP16 construct and transfected with pAP17 (Fig. 2d). More importantly, the wild type chimera had no detectable capacity to transactivate pTK-CAT reporter devoid of EVI1 consensus binding sites (Fig. 2d). To test the regulation of EVI1-VP16 transactivation activity by tet, we transfected the pAP17 reporter into S2-6, 6D, and RN13 cells grown with or without tet. This clearly showed that the 6D cell line has CAT activity only upon removal of tet; in contrast S2-6 and RN13 had no CAT activity, with or without tet (Fig. 2e).

*Microarray Analysis of Gene Expression in Tet-inducible Clones Expressing Wild Type and Mutant EVI1-VP16*—The reporter assays (Fig. 2) indicated that nonmutant EVI1-VP16 was capable of activating the pAP17 reporter, whereas the EVI1<sup>R205N</sup>-VP16 mutant was not. It has been shown that the

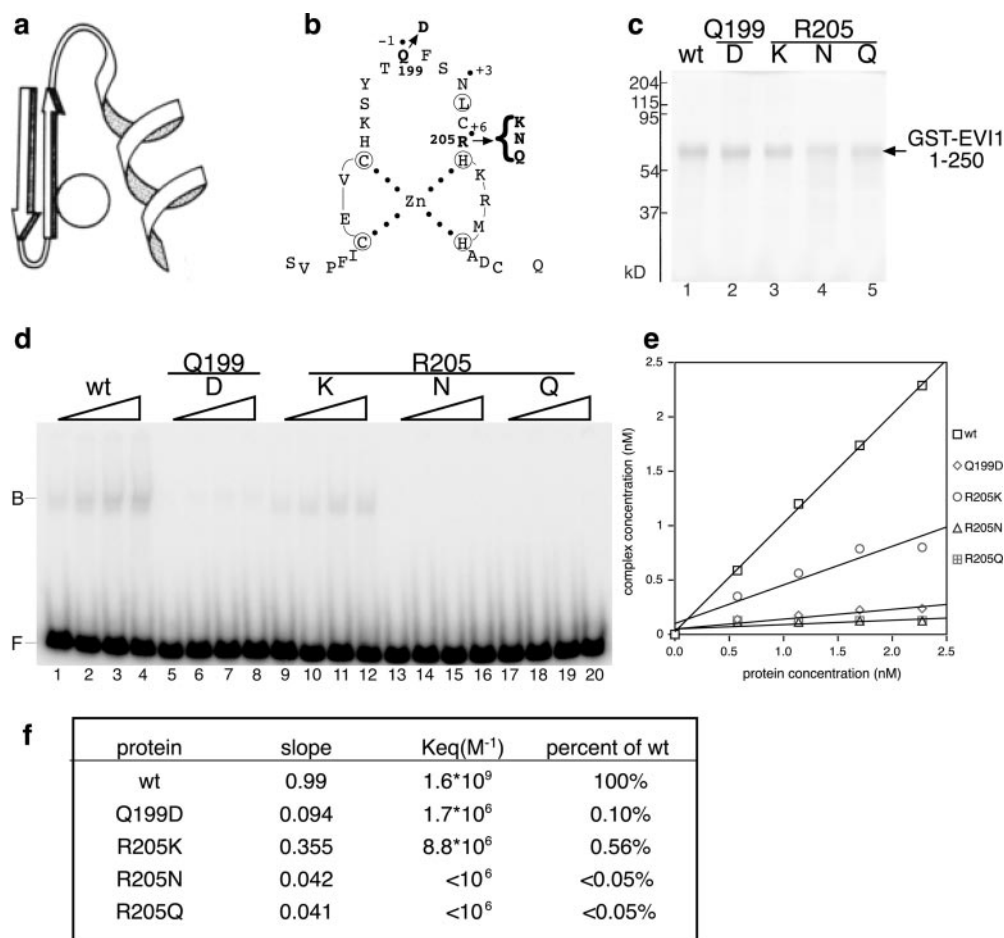


**FIG. 1. Generation of EVI1 mutants defective in specific DNA binding.** *a*, ribbon structure of zinc finger protein (used with permission from J. M. Berg (10)), showing the N-terminal antiparallel  $\beta$ -sheet structure and C-terminal  $\alpha$ -helical region. *b*, amino acid sequence of zinc finger 6, depicting the residues altered by mutagenesis (in **boldface**): Gln<sup>199</sup> and Arg<sup>205</sup>. The numbers -1, +3, and +6 refer to positions along the  $\alpha$ -helix; *dotted* residues are those putatively involved in providing DNA contacts. *c*, Coomassie Blue-stained SDS-PAGE gel analysis of purified GST fusion proteins: wild type (*wt*) EVI1-(1-249) (lane 1); Q199D (lane 2); R205K (lane 3); R205N (lane 4); and R205Q (lane 5). *d*, electromobility shift assay performed with a radiolabeled probe containing the EVI1-binding site, with titration of proteins to determine  $K_{eq}$  for protein-DNA binding. Samples are as indicated above each set of four lanes; protein amounts increase from 11.25 to 45 fmol across the four lanes. *B* indicates probe bound to protein; *F* denotes free probe. *e*, graph depicting the relationship between protein concentration (*x* axis) and protein-DNA complex concentration for wild type and mutant GST fusion proteins; data are derived from EMSA in *d*. *f*, table showing the derivation of  $K_{eq}$  for each of the samples tested. The  $K_{eq}$  was derived using the slope derived from the graph in *e* and the equation under "Experimental Procedures" (derived from Ref. 32) and is expressed as  $M^{-1}$  and as a percentage of the wild type affinity.

ability of EVI1 to transform cells depends on the first set of zinc fingers (13), and this is likely through the effects of EVI1 binding to specific GACAAGATA-like sites in the genome, modulating the expression of genes located in *cis*. Therefore, of obvious interest are the locations of these binding sites and the identity of EVI1 target genes. A standard approach to target gene identification is to induce the expression of the transcription factor in question and to document changes in gene expression by microarray. However, in assays using synthetic reporters, EVI1 is a repressor (23), and identification of target genes of repressors is more problematic than finding targets of activators, because it requires that the gene be "on" prior to induction of the repressor (which may not be the case in a particular cell line) and because repression of a gene with low basal level of expression would be hard to detect. The EVI1-VP16 chimera possesses the DNA binding specificity of EVI1 and can activate EVI1 reporter genes (Fig. 2) and presumably EVI1 target genes (22). We hypothesized that this approach would likely be more robust than trying to identify genes repressed by full-length EVI1. To determine whether this was the case, we performed differential mRNA expression profiling to identify genes up-regulated by EVI1-VP16. Thus, we induced EVI1-VP16 expression in the 6D cell line (Table IV) by tet

removal and harvested RNA, and we used this for microarray analysis in a competitive hybridization with labeled cDNA derived from RNA from induced S2-6 cells (the parental cell line for 6D, harboring the autoregulated TetR-VP16 only and lacking EVI1-VP16; see Table IV). As additional controls in the gene expression profiling, we performed competitive hybridizations comparing labeled cDNA derived from induced 6D RNA to the same from induced RN13 cells, containing the EVI1<sup>R205N</sup>-VP16 chimera (Table IV). This control was designed to eliminate the identification of genes induced by tet itself or by TetR-VP16, as well as genes induced via effects of EVI1-VP16 that are not dependent on high affinity binding of the chimera to DNA.

For gene expression profiling, glass slide-based oligonucleotide arrays of sequences for 13,400 mouse genes were employed. All samples were obtained from cells induced by removal of tet for 15 h, at which time activation of expression of endogenous genes by EVI1-VP16 is clearly evident (data not shown). Data were collected from four hybridizations (two comparing 6D and S2-6 and two comparing 6D and RN13) and identification of the induced genes was based on fold change and *t* test. Analysis of the 6D *versus* RN13 revealed 185 genes were induced; in the 6D *versus* S2-6 experiment, 61 genes were

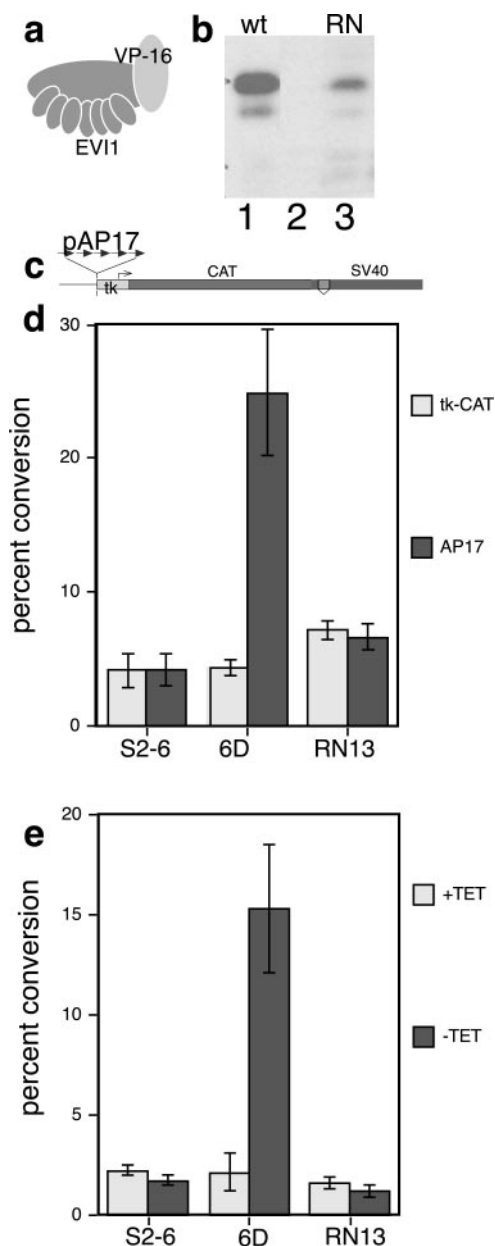


**FIG. 2. *In vivo* assessment of DNA binding to GACAAGATA motif by wild type and mutant EVI1-VP16 constructs.** *a*, schematic depicting the EVI1-VP16 chimera. *b*, Western blot analysis of protein extracts from induced cells, either 6D (lane 1), S2-6 control (lane 2), or RN13 (lane 3), using anti-N-terminal EVI1 antiserum to detect proteins. *wt*, wild type. *c*, schematic showing the structure of the pAP17 reporter, comprised of the basal promoter of the herpes simplex virus tk gene (*tk*) linked to CAT, with a SV40 splice and polyadenylation sequence. The five arrows above the *tk* segment indicate the pentameric GACAAGATA motif. The pTK-CAT reporter is the same but is lacking the GACAAGATA motif. *d*, results of CAT reporter assay, performed in induced S2-6, 6D cells, or RN13, as indicated. Transfected reporter plasmids are either pAP17 or pTK-CAT, as indicated. The data are normalized to the activity of a cotransfected  $\beta$ -galactosidase gene and are expressed relative to the S2-6/pTK-CAT control. *e*, CAT assay of induced ( $-TET$ ) and uninduced ( $+TET$ ) S2-6, 6D, and RN13, as indicated, transfected with the AP17 reporter.

induced; 22 of these were induced in both hybridizations. These 22 were subjected to further analysis.

To address further whether some of these genes could have been induced nonspecifically by EVI1-VP16 by an activity independent of binding to DNA, such as squelching of transcription cofactors or titration of repressors, we performed an additional set of hybridizations comparing RNA from uninduced

TABLE IV  
Cell lines used in this study

Cell line	Regulated gene	Mutation in EVI1
S2-6	None	NA
6D	EVI1-VP16	None
RN13	EVI1-VP16	R205N
718	135-kDa EVI1-HA	None
NFS58	None; proviral insertion at <i>Evi1</i>	None
32Dcl3	None; proviral insertion at <i>Evi1</i>	None

EVI1<sup>R205N</sup>-VP16 against RNA from the same cell line induced for 15 h. This comparison should reveal genes that are induced but not due to the binding of the chimera to the DNA because EVI1<sup>R205N</sup>-VP16 is incapable of significant DNA binding. In addition, because the two cell lines, 6D and RN13, express different levels of protein upon induction (Fig. 2), the comparison of RN13 induced *versus* uninduced will reveal genes that were induced by both 6D and RN13, but to a greater extent in 6D because of the higher level of expression. We performed this hybridization twice. Based on these data, we elected to disregard genes with inductions greater than 2-fold with EVI1<sup>R205N</sup>-VP16. This eliminated six genes, leaving 16 genes for which the average fold change of gene expression upon induction of EVI1<sup>R205N</sup>-VP16 is listed in the columns to the right in Table V. Also shown in Table V are the *p* values derived from the Student's *t* test, comparing the normalized pixel values for the control samples (S2-6 or RN13) to the experimental samples (6D) in a pairwise manner. The *p* values ranged from 0.002 to 0.042, with a median of 0.009; 9 of the 16 genes were significant to  $p \leq 0.01$ ; for 5 other genes,  $0.01 < p < 0.02$  (Table V).

The EVI1-VP16-responsive genes represent an interesting set, encoding transcription factors (GATA2, GATA3, Klf5 (BTEB2), Zfpm2 (FOG2), Skil, and Plagl1), a signaling molecule (Map3k14), and an extracellular matrix component (Dcn).

**Quantitation of mRNA Levels by Real Time PCR**—To confirm the microarray results, we performed quantitative real time PCR using the intercalating dye SybrGreen to detect the accumulation of double-strand products in the PCR. Reactions were performed to compare uninduced 6D cells to induced 6D cells. For all nine genes tested, quantitative PCR showed fold inductions of comparable size to that seen by microarray: *Gadd45g* 4.3-fold induced; *Gata2* was 2.0-fold; *Gata3* 3.7-fold; *Klf5* 4.7-fold; *Map3k14* 4.3-fold; *Napb* 7.0-fold. *Skil* 4.6-fold, *Tnnt2* 8.6-fold; and *Zfpm2* 3.7-fold. All values are normalized to  $\beta$ -actin. These data are summarized in Table V.

**Analysis of Gene Promoter Regions Reveals Evolutionarily Conserved EVI1-binding Sites**—The microarray data demonstrate that 16 genes are specifically up-regulated by EVI1-VP16, but not by mutant EVI1<sup>R205N</sup>-VP16 defective in DNA binding. We predicted that there would be EVI1-binding sites located in *cis* near the transcription start sites (TSS) for these genes. To obtain data in support of this, we retrieved DNA sequences located within 10 kb of the TSS from mouse and human genomic sequence, and we performed DNA sequence alignment and searches for GACAAGATA-like EVI1-binding sites. The location of the TSS was based on the 5' extent of the "reference sequence" (RefSeq) available at the EntrezGene site for each gene ([www.ncbi.nih.gov/entrez/query.fcgi?db = gene](http://www.ncbi.nih.gov/entrez/query.fcgi?db= gene)). Alignments were accomplished using DNA analysis software Megalign, and the identification of EVI1-binding sites was done using the TFSEARCH program ([www.cbrc.jp/research/db/TFSEARCH.html](http://www.cbrc.jp/research/db/TFSEARCH.html)). The locations of binding sites were superimposed on the DNA sequence alignments to reveal the relative location of potential functional sequence motifs. A representative analysis is shown in Fig. 3 for the putative target gene *Dcn*. This analysis was done for 12 of the 16 genes in Table V, and

TABLE V  
Genes induced by EVI1-(1-250)-VP16

No.	DNA_ID	Annotation	Gene symbol	Fold induced	Quantitative-PCR <sup>a</sup>	t test	Log <sub>2</sub> RN13 (IU) <sup>b</sup>
1	AK011986	RIKEN cDNA 2610305D13 gene	<i>2610305D13Rik</i>	6.17		0.009	0.440
2	AK019665	RIKEN cDNA 4930503B16 gene	<i>4930503B16Rik</i>	3.54		0.009	-0.413
3	AK015913	RIKEN cDNA 4930527E24 gene	<i>4930527E24Rik</i>	3.26		0.014	0.306
4	X53929	Decorin	<i>Dcn</i>	3.84		0.015	-0.064
5	AK002979	Dopamine receptor D1 interacting protein	<i>Drd1ip</i>	3.15		0.011	0.612
6	AF055638	Growth arrest and DNA damage-inducible, $\gamma$	<i>Gadd45g</i>	6.83	4.3	0.003	0.860
7	NM_008090	GATA-binding protein 2	<i>Gata2</i>	2.0	2.0	0.010	0.420
8	X55123	GATA-binding protein 3	<i>Gata3</i>	4.31	3.7	0.042	0.333
9	AB025099	Basic transcription element-binding protein 2	<i>Klf5</i>	2.98	4.7	0.026	-0.163
10	AF143094	NF- $\kappa$ B-inducing kinase	<i>Map3k14</i>	5.11	4.3	0.025	0.000
11	X61450	N-Ethylmaleimide-sensitive fusion protein attachment protein $\beta$	<i>Napb</i>	2.80	7.0	0.002	0.793
12	AF147785	Pleiomorphic adenoma gene-like 1	<i>Plagl1</i>	4.15		0.017	0.159
13	U10532	Ski/sno-related	<i>Skil</i>	4.26	4.6	0.008	-0.353
14	L47570	Troponin T2, cardiac	<i>Tnnt2</i>	3.02	8.6	0.004	0.284
15	X72697	Xlr-related, meiosis-regulated	<i>Xmr</i>	6.58		0.004	0.000
16	AF125166	Zinc finger protein, multitype 2	<i>Zfpm2</i>	3.78	3.7	0.015	0.000

<sup>a</sup> Fold induction (6D, induced/uninduced), normalized for  $\beta$ -actin.

<sup>b</sup> Log<sub>2</sub> of the ratio of level of gene expression in RN13 cells, induced/uninduced.

the putative binding sites identified are tabulated in Table VI.

**ChIP Reveals Occupancy of EVI1 on GACAAGATA-like Motifs Near Several Putative Target Genes**—To test if EVI1 binds to the evolutionarily conserved GACAAGATA-like motifs located near genes that are up-regulated by EVI1-VP16, we performed chromatin immunoprecipitation experiments. Two antisera against EVI1 were generated as follows: one directed against the N terminus (amino acids Met<sup>1</sup>–Gly<sup>249</sup>) and the other against the C terminus (amino acids Lys<sup>719</sup>–Pro<sup>734</sup> and Asn<sup>805</sup>–Val<sup>1042</sup>).

In initial experiments, the ability of our antiserum against the N terminus of EVI1 to immunoprecipitate EVI1 was tested. An S2-6-derived cell line was created with a hemagglutinin-tagged version of the 135-kDa EVI1 cDNA under the control of tet operons (cell line 718; Table IV). Removal of tetracycline resulted in expression of the appropriate-sized protein, detectable with anti-N-terminal EVI1 antiserum (Fig. 4A, lanes 1 and 2). This antiserum was then tested for its ability to immunoprecipitate HA-tagged EVI1 from induced 718 cells. Induced 718 cells were lysed, incubated with anti-N-terminal antiserum, and precipitated with protein A-Sepharose. Precipitated proteins were fractionated on SDS-PAGE and analyzed by Western blot using anti-HA antibody (Fig. 4A, lane 3). The presence of a band of the correct molecular weight that is detectable with HA antibody indicates that the anti-N-terminal antiserum is able to immunoprecipitate EVI1 protein. In this experiment, a C terminus-specific anti-EVI1 antiserum was also shown to be able to precipitate EVI1 (Fig. 4A, lane 4).

To test if the N terminus-specific anti-EVI1 antiserum could be used for chromatin immunoprecipitation, we first created a test cell line by transfecting pAP17, the CAT reporter plasmid bearing five EVI1-binding sites within the promoter (Fig. 2c), into 6D cells, which harbor the tet-regulated EVI1-VP16 (Table IV). Single cell-derived clones were tested for the responsiveness of pAP17 to EVI1-VP16 by removing tet and assaying for CAT activity. Several clones proved positive, showing CAT activity without tet but not with tet (data not shown). Cell extracts from control transfections (pTK-CAT reporter into 6D cells and pAP17 into parental S2-6 cells) showed no CAT activity (data not shown). We then performed ChIP on 6D + pAP17 clone A, one of the derivative lines showing CAT activity, as well as on pooled 6D + pAP17 cells. Cells were grown either with or without tet and harvested, and the cross-linked chromatin was immunoprecipitated with the N terminus-specific anti-EVI1. The immunoprecipitated material was ampli-

fied with primers specific for the TK promoter region of the CAT reporter that flank the EVI1-binding sites. In parallel, control precipitations of cross-linked chromatin were performed with no primary antiserum, and this material was probed as well by PCR with the same primers. A specific PCR product was present only when immunoprecipitations were performed with anti-EVI1 antiserum using chromatin obtained from induced 6D cells in which EVI1-VP16 is expressed (Fig. 4, B, lane 6, and C, lane 7). Parallel reactions with material from uninduced cells (Fig. 4, B, lane 3, and C, lane 4) and immunoprecipitations with no antiserum (Fig. 4, B, lane 5, and C, lane 6) showed no specific product. These data clearly indicate that EVI1-VP16 is occupying the EVI1-binding sites within the transfected pAP17 reporter within induced 6D cells, and also provide evidence that our anti-EVI1 antiserum could successfully immunoprecipitate EVI1.

By using this immunoprecipitated material, we then performed PCR for putative EVI1-binding sites near induced genes (Fig. 5; Table VI). By using ChIP, we revealed EVI1 binding to 12 sites within 10 of the 12 genes tested. These were *Dcn*, *Drd1ip*, *Gadd45g*, *Gata2*, *Klf5*, *Map3K14*, *Napb*, *Skil*, *Tnnt2*, and *Zfpm2*. Some genes, such as *Zfpm2* and *Skil* were shown to possess two binding sites for EVI1-VP16. For the two genes for which EVI1-VP16 binding was not detected (*Gata3* and *Plagl1*), it is possible that there is binding to other GACAAGATA-like motifs that were not chosen for ChIP analysis.

**ChIP Analysis of EVI1-expressing Myeloid Cells 32Dcl3 and NFS58 Reveals Significant Binding to the Same Sites Identified in Fibroblasts**—Of obvious interest is the location of EVI1-binding sites in myeloid cells that overexpress EVI1, because it is possible that genes located in *cis* to these sites are regulated by EVI1 and that their deregulation (either suppression or activation) by EVI1 plays a role in the biologic effects of EVI1 on myeloid cells. Thus, we performed ChIP analysis on myeloid cell lines that harbor proviral insertions at EVI1. Considering it likely that the level of EVI1 in the cell would influence the degree to which genomic binding sites are occupied (e.g. as is true for c-Myc (41)), we screened cell lines with proviral insertions at EVI1 for their level of EVI1 mRNA transcript by quantitative PCR (Table VII). This revealed a spectrum of expression levels, but all were markedly higher than FDCP-GM cells that lack a proviral insertion at *Evi1*. We chose two cell lines, one leukemic (NFS58 (1)) and one nonleukemic (32Dcl3 (42)) for ChIP analysis, both of which express signifi-

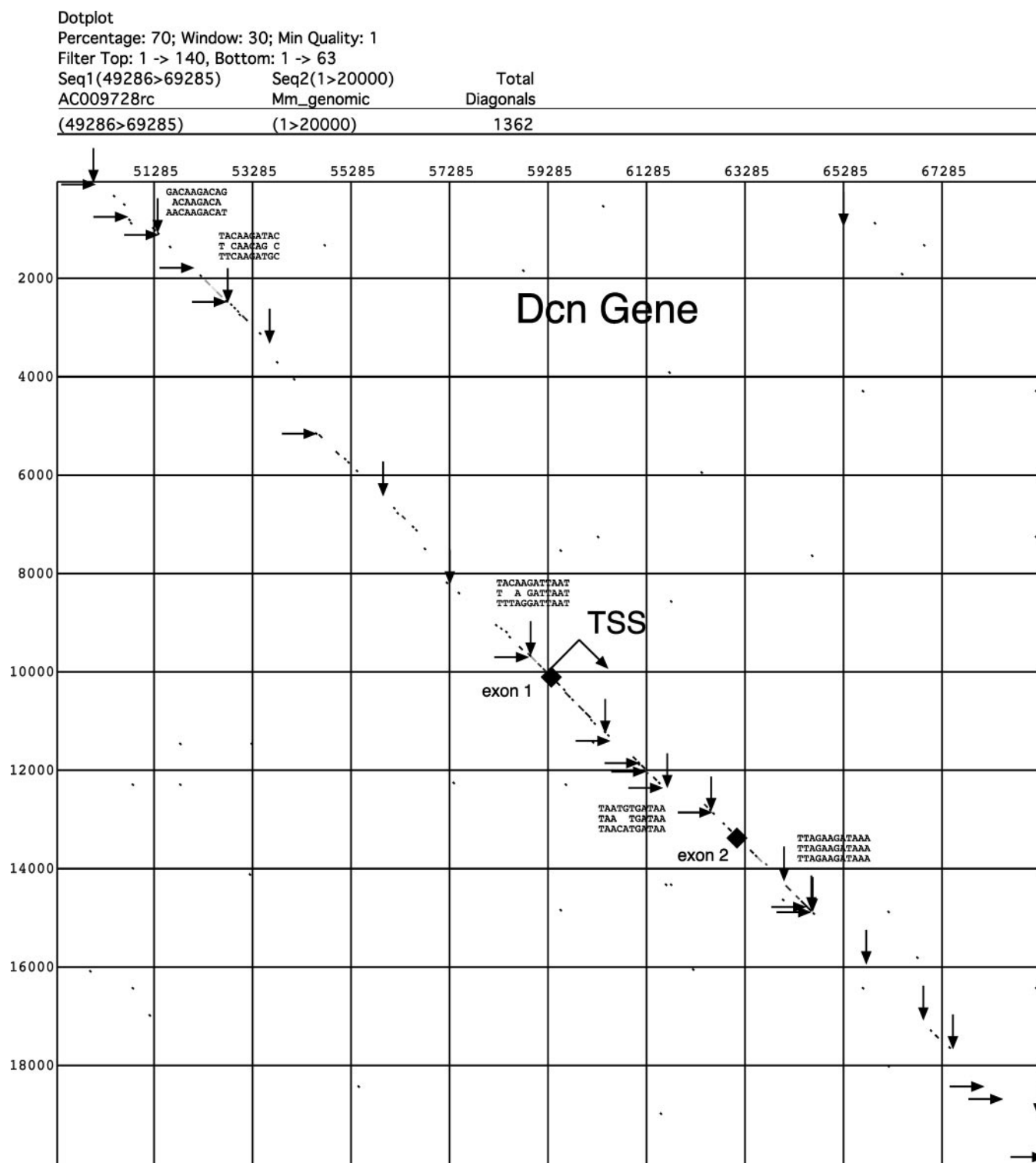


FIG. 3. **Analysis of *Dcn* gene for EVI1-binding sites.** Alignment of 10,000 bp of the human (x axis) and mouse (y axis) sequence surrounding the transcription start site (TSS, as indicated) of the *Dcn* gene. Locations of exons 1 and 2 are shown. Vertical arrows denote the location of GACAAGATA-like motifs (as identified by TFSEARCH algorithm) in mouse DNA, and horizontal arrows indicate the ones found in human DNA. The alignments for five evolutionarily conserved sites are shown, where the top line is mouse; the bottom line is human; and the middle line represents identical bases.

cant levels of EVI1 RNA, with NFS58 expressing 4.3 times higher levels than 32Dcl3 cells (Table VII).

Immunoprecipitations of cross-linked chromatin from NFS58 and 32Dcl3 cells were performed with both N terminus-specific and C terminus-specific antisera, whereas control precipitations were conducted with normal rabbit serum. Results indicate that for many of the sites tested, there was occupancy

by EVI1 in NFS58 and 32Dcl3 cells, with that occupancy being generally higher in NFS58 cells than 32Dcl3 cells, correlating with the higher level of EVI1 expression in NFS58 cells (Fig. 5). In general, the results in NFS58 paralleled those obtained in 6D cells. At sites where occupancy was high in 6D cells (as reflected by an abundant PCR product), there tended to be more product in NFS58 cells as well (e.g. *Gadd45g* + 2500,

TABLE VI  
Chromatin immunoprecipitation, PCR results

Gene	Location of site	Binding site	6D cells	NFS58	32Dc13
<i>Dcn</i>	+4785	AGAAGATAAA	++	+/-	+/-
<i>Drd1ip</i>	-7993	ACAAAATAA	+++	++	+/-
<i>Gadd45g</i>	+2543	AAAAGATAA	+++	+++	++
<i>Gadd45g</i>	-4827	AAGATAAGCTA	-	-	-
<i>Gata2</i>	-2880	AGATAAGAAAC	++	+++	++
<i>Gata3</i>	-7200	GACAAGATA	-	-	-
<i>Klf5</i>	-3100	AGAGAAGATAC	++	-	ND <sup>a</sup>
<i>Map3K14</i>	-2666	ACAAGATGA	+++	++	-
<i>Napb</i>	-8829	AGATAAGATAT	+++	+++	+++
<i>Plagl1</i>	+1771	CACAAGATAA	-	-	-
<i>Skil</i>	+1425	TGACAAGAGAA	+++	+++	+++
<i>Skil</i>	+5400	CAGAGAAGATA	+++	++	ND
<i>Tnnt2</i>	+5762	AGAAAAGATAA	+++	+/-	-
<i>Zfpm2</i>	-954	GACAAGATCA	-	-	-
<i>Zfpm2</i>	-2500	ACAAAATAA	+	+/-	-
<i>Zfpm2</i>	-3200	ACAAGATAT	+++	++	-

<sup>a</sup> ND indicates not determined.

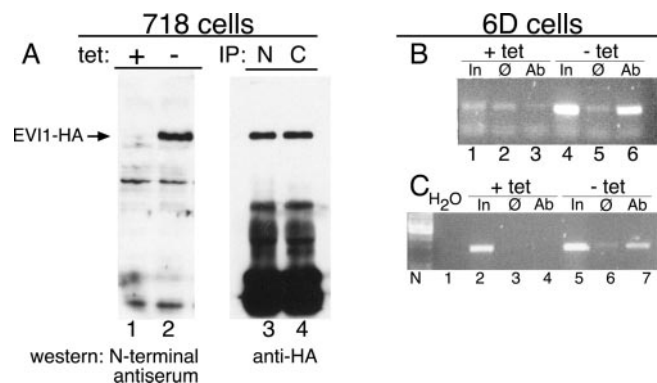


FIG. 4. Chromatin immunoprecipitation, assessment of anti-ara and demonstration of binding of EVI1-VP16 to GACAA-GATA in CAT reporter. A, Western blot analysis of uninduced (lane 1) and induced (lane 2) 718 cells, expressing full-length 135-kDa EVI1-HA, detected with N terminus-specific anti-EVI1 antiserum. In lanes 3 and 4, proteins are precipitated from extracts prepared from 718 cells with N terminus-specific (N) and C terminus-specific (C) antisera, respectively, and then analyzed by Western blot analysis with anti-HA antibody. B and C, ethidium bromide-stained agarose gel electrophoresis of products of PCRs using primers that flank the EVI1-binding sites in the pAP17 reporter, which has been transferred into 6D cells as a stable locus. Prior to harvest, cells were either induced (-tet) or left uninduced (+tet) to increase expression of EVI1-VP16. Chromatin was precipitated with no primary antiserum (lanes denoted Ø) or with antiserum specific for the N terminus of EVI1 (lanes marked Ab). In denotes a 1:100 dilution of the DNA sample put into the immunoprecipitation reaction. B and C represent results from experiments performed with 6D + pAP17 clone A and 6D + pAP17 pooled cells, respectively.

*Napb*, *Skil* + 1400). For those sites with little or no binding in 6D cells, there was a similarly negative result in NFS58 cells (e.g. *Gata3* and *Plagl1*). For some sites, like *Gata2*-3000 and *Zfpm2*-3200, the N-terminal antibody resulted in a higher amount of PCR product than the C-terminal antibody, but in general, there was congruence in the results obtained with the two antisera. Overall, 12 of the 15 sites exhibited some level of occupancy by EVI1 in NFS58 cells, whereas 6 of 13 were positive at some level in 32Dc13 cells.

#### DISCUSSION

We describe an innovative screen for putative EVI1 target genes that involves an inducible EVI1-VP16 chimera that has the binding specificity of EVI1 yet can activate endogenous genes. This tool allows us to circumvent the problem that the normal EVI1 protein can either activate or repress synthetic reporter constructs, depending on the EVI1-binding sites within the reporter (23, 25). EVI1 is known to repress certain

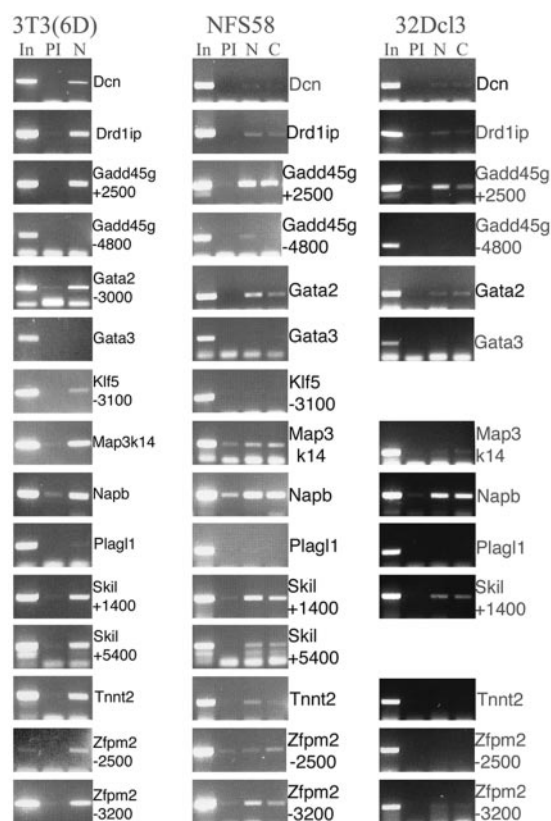


FIG. 5. Chromatin immunoprecipitation to demonstrate binding of EVI1-VP16 or EVI1 to regions containing GACAA-GATA-like motifs, located near regulated genes. Ethidium bromide-stained agarose gel electrophoresis of products from PCRs for the regions indicated, to test their immunoprecipitation with anti-EVI1 antiserum (N-terminal-specific, denoted by N, or C-terminal-specific, denoted by C). Figure shows ChIP analysis of EVI1-VP16 binding in induced 6D cells (left column), NFS58 cells (middle column), and 32Dc13 cells (right column) using for immunoprecipitation either normal rabbit antiserum (denoted PI) or antiserum specific for EVI1 for immunoprecipitation (N or C terminus-specific). In denotes input DNA.

reporters, an activity that is mediated at least in part through an interaction with CtBP through a PLDLS motif (28). However, in the EVI1-VP16 chimera, this site is absent, and we have tethered the EVI1 DNA binding domain located in amino acids 1-250 to the activation domain of the herpes simplex virus VP16 protein. In this paper, we show that in addition to activating synthetic reporter constructs, this chimera can also activate expression of endogenous genes. This general ap-

TABLE VII  
*Evi1*, quantitative reverse transcription-PCR

Values are relative to a control RNA sample from normal mouse kidney.

Sample	Proviral insertion at <i>Evi1</i>	Exp. 1	Exp. 2	Exp. 3	Average
32Dcl3	+	13.8	10.1	12.9	12.3
DA-1	+	31.4	18.5	20.9	23.6
NFS-58	+	47.0	58.8	52.8	52.9
NFS-60	+	4.4	8.0	8.1	6.8
NFS-78	+	43.1	87.8	65.6	65.5
FDCP-GM	–	1.3	1.3	1.2	1.3

proach could potentially be used to identify target genes for other DNA binding transcriptional repressors.

Our goal in this study is to identify candidate EVI1 target genes that may play a role in EVI1-induced transformation. Whether the genes identified in this study are physiologic targets of EVI1 is not clear and will be the subject of future work. What is provided here is a screen for genes that are likely regulated by EVI1 in some context; we have shown that EVI1 isoforms occupy GACAAGATA-like motifs within 10 kb of the TSS of 6–10 of the 12 putative targets tested, consistent with their being regulated by EVI1. It is likely that some of these function as EVI1 targets only within specific cell types, *e.g.* *Tnn2* within the heart and *Drd1ip* within the brain.

A critical question is the role that these genes play in EVI1-induced transformation, which is currently under study. In Rat1 fibroblasts, EVI1 has been shown to accelerate the cell cycle, an activity that requires the N-terminal zinc finger domain (12). We have demonstrated that the ability of EVI1 to transform Rat1 cells to anchorage independence depends on its ability to bind DNA, because the R205N mutation is devoid of transforming activity.<sup>4</sup> This suggests that EVI1 works through its binding to genomic sites and modulation of target genes in order to induce transformation. Noticeably absent in our list of targets are any genes that are directly involved in the regulation of cell cycle or growth arrest, such as cyclin genes. However, some of the putative targets identified are regulators of such genes. For instance, *Skil* (*SnoN*) is closely related to the protooncogene *c-ski* and can transform cells in culture (43). It is overexpressed in a wide variety of cancers and blocks TGF $\beta$  signaling, which is a negative regulator of cell proliferation. Most interestingly, mice heterozygous for deletion of *Skil* are hypersensitive to chemical carcinogen-induced tumors, suggesting *Skil* can also act as a tumor suppressor gene (44), a result that has not been reconciled with the effect of *Skil* on TGF $\beta$  signaling and cell cycle. SKIL/SnoN protein has been found to interact with Smad proteins, which mediate the transcriptional effects of TGF $\beta$  upon receptor activation, and thereby negatively regulate TGF $\beta$  signaling (45). Key targets of Smad action are the cell cycle inhibitors p21<sup>CIP1</sup> and p15<sup>INK4B</sup> (46, 47). SKIL/SnoN, through disruption of functional Smad complexes, causes transformation (48) most likely, at least in part, through a decrease in these cell cycle inhibitors, resulting in cell cycle progression. Studies have shown that high level expression of the 135-kDa isoform of EVI1 interferes with the growth inhibitory effects of TGF $\beta$ . Expression of this isoform represses TGF $\beta$ -mediated transactivation of a TGF $\beta$  reporter and leads to diminished responsiveness of the growth inhibitory effects of TGF $\beta$  (49, 50). This repressive effect is mediated by EVI1 zinc fingers 1–7, perhaps through interaction with Smad3 (49), because deletions of broad and nonoverlapping sections of this region result in loss of the ability to inhibit TGF $\beta$  activation of reporters and loss of ability to interact with SMAD3 (49). However, it may also be that EVI1 inhibits TGF $\beta$

signaling through an increase in *Skil/SnoN* expression. Whether these effects are critical to leukemogenesis is not clear, because several myeloid cell lines that express *Evi1* because of proviral insertion, such as NFS60 (1) and 32Dcl3 (42), have been shown to be sensitive to the growth inhibitory effects of TGF $\beta$  (51). However, EVI1 is expressed in various tissues in the developing mouse (52), and it may be that within this context EVI1 inhibits TGF $\beta$  signaling.

Two *Gata* genes, *Gata2* and *Gata3*, were identified as potential target genes, as well as a GATA-binding protein FOG2 (encoded by *Zfpm2*). EVI1 binding near *Gata2* and *Zfpm2* was confirmed by chromatin immunoprecipitation, whereas the binding sites near *Gata3* are as yet unidentified. The possibility that EVI1 may regulate *Gata2* expression may yield insight into EVI1-induced leukemias. *Gata2* is highly expressed in primitive hematopoietic cells, but its expression diminishes upon differentiation (53). Its importance as a key regulator of early hematopoiesis is illustrated by the phenotype of the *Gata2* knock-out mouse, which has profound defects in definitive hematopoiesis (54). *Gata2* is known to be expressed in the EVI1-expressing myeloid progenitor cell line 32Dcl3, and *EVI1* has been shown to be expressed in hematopoietic progenitors, the same cells that express *GATA2* (55).<sup>5</sup> *GATA2* is expressed in 87% of *de novo* cases of acute myelogenous leukemia (56), and a dominant-negative form of *Gata3* (which also blocks *GATA2* function) is able to overcome activated Notch-induced block to differentiation (57), suggesting it plays a key role in the differentiation block caused by activated Notch. *Gata2* also inhibits the differentiation of progenitors into erythroid cells, while promoting their differentiation into megakaryocytic cells (58), which are two activities that have been shown for *Evi1* (8, 59). In *Evi1*<sup>−/−</sup> embryos, *Gata2* expression is markedly reduced, and restoration of *Gata2* corrected a proliferative defect in *Evi1*<sup>−/−</sup> hematopoietic precursors, suggesting that *Gata2* is a critical target of *Evi1* (60). It is possible that transcriptional activation of *Gata2* contributes, in part, to EVI1-induced block to myeloid and erythroid differentiation (9) and cell proliferation. However, in cells programmed to overexpress *Gata2*, cell proliferation appears to be inhibited (61).

In summary, we have provided a set of 16 potential target genes, and we further demonstrate that EVI1 can bind to 10 of these genes *in vivo*. These data provide a starting point for further studies aimed at uncovering the mechanism for EVI1-induced transformation.

*Acknowledgments*—We thank Hong Sun for excellent technical assistance in performing the oligonucleotide microarrays. We also thank Donald Crothers, Ann Valentine, Diane S. Krause, and Bernard G. Forget for their comments on this manuscript. We thank Jeremy Berg for granting permission to use the ribbon structure of a zinc finger depicted in Fig. 1a. The Keck DNA Microarray Resource at Yale Uni-

<sup>4</sup> B. Yatsula, S. Lin, A. J. Read, J. Wheeler, D. Tuck, and A. S. Perkins, manuscript in preparation.

<sup>5</sup> K. Lezon-Geyda, S. Lin, B. Yatsula, C. Galvuo, G. Steele-Perkins, M. C. Lopingco, F. Sigurdsson, N. Berliner, F. Camargo, and A. S. Perkins, manuscript in preparation.

versity is supported by the Anna and Argall Hull Fund, the NIH/NIDDK Microarray Biotechnology Center Grant (NIH 5 u24 DK58776; principal investigator Kenneth Williams), the C. G. Swebilius Trust U. W., and the Yale University Department of Pathology.

## REFERENCES

- Morishita, K., Parker, D. S., Mucenski, M. L., Jenkins, N. A., Copeland, N. G., and Ihle, J. N. (1988) *Cell* **54**, 831–840
- Bartholomew, C., Morishita, K., Askew, D., Buchberg, D., Jenkins, N. A., Copeland, N. G., and Ihle, J. N. (1989) *Oncogene* **4**, 529–534
- Fichelson, S., Dreyfus, F., Berger, R., Melle, J., Bastard, C., Miclea, J., and Gisselbrecht, S. (1992) *Leukemia (Baltimore)* **6**, 93–99
- Mitani, K., Ogawa, S., Tanaka, T., Miyoshi, H., Kurokawa, M., Mano, H., Yazaki, Y., Ohki, M., and Hirai, H. (1994) *EMBO J.* **13**, 504–510
- Morishita, K., Parganas, E., Willman, C. L., Whittaker, M. H., Drabkin, H., Oval, J., Taetle, R., Valentine, M. B., and Ihle, J. N. (1992) *Proc. Natl. Acad. Sci. U. S. A.* **89**, 3937–3941
- Nucifora, G., Begy, C., Kobayashi, H., Roulston, D., Claxton, D., Pedersen-Bjergaard, J., Parganas, E., Ihle, J., and Rowley, J. (1994) *Proc. Natl. Acad. Sci. U. S. A.* **91**, 4004–4008
- Suzukawa, K., Parganas, E., Gajjar, A., Abe, T., Takahashi, S., Tani, K., Asano, S., Asou, H., Kamada, N., Yokota, J., Morishita, K., and Ihle, J. N. (1994) *Blood* **84**, 2681–2688
- Kreider, B., Orkin, S., and Ihle, J. (1993) *Proc. Natl. Acad. Sci. U. S. A.* **90**, 6454–6458
- Morishita, K., Parganas, E., Matsugi, T., and Ihle, J. N. (1992) *Mol. Cell. Biol.* **12**, 183–189
- Berg, J. (1988) *Proc. Natl. Acad. Sci. U. S. A.* **85**, 99–102
- Chi, Y., Senyuk, V., Chakraborty, S., and Nucifora, G. (2003) *J. Biol. Chem.* **278**, 49806–49811
- Kilbey, A., Stephens, V., and Bartholomew, C. (1999) *Cell Growth Differ.* **10**, 601–610
- Kilbey, A., and Bartholomew, C. (1998) *Oncogene* **16**, 2287–2291
- Kurokawa, M., Ogawa, S., Tanaka, T., Mitani, K., Yazaki, Y., Witte, O., and Hirai, H. (1995) *Oncogene* **11**, 833–840
- Bordereaux, D., Fichelson, S., Tambourin, P., and Gisselbrecht, S. (1990) *Oncogene* **5**, 925–927
- Morishita, K., Parganas, E., Douglass, E. C., and Ihle, J. N. (1990) *Oncogene* **5**, 963–971
- Bartholomew, C., and Clark, A. M. (1994) *Oncogene* **9**, 939–942
- Fears, S., Mathieu, C., Zeleznick-Le, N., Huang, S., Rowley, J., and Nucifora, G. (1996) *Proc. Natl. Acad. Sci. U. S. A.* **93**, 1642–1647
- Perkins, A. S., Fishel, R., Jenkins, N. A., and Copeland, N. G. (1991) *Mol. Cell. Biol.* **11**, 2665–2674
- Delwel, R., Funabiki, T., Kreider, B., Morishita, K., and Ihle, J. (1993) *Mol. Cell. Biol.* **13**, 4291–4300
- Funabiki, T., Kreider, B. L., and Ihle, J. N. (1994) *Oncogene* **9**, 1575–1581
- Kim, J., Hui, P., Yue, D., Aycock, J., Leclerc, C., Björing, A., and Perkins, A. (1998) *Oncogene* **17**, 1527–1538
- Perkins, A., and Kim, J. (1996) *J. Biol. Chem.* **271**, 1104–1110
- Bartholomew, C., Kilbey, A., Clark, A., and Walker, M. (1997) *Oncogene* **14**, 569–577
- Morishita, K., Suzukawa, K., Taki, T., Ihle, J. N., and Yokota, J. (1995) *Oncogene* **10**, 1961–1967
- Tanaka, T., Nishida, J., Mitani, K., Ogawa, S., Yazaki, Y., and Hirai, H. (1994) *J. Biol. Chem.* **269**, 24020–24026
- Turner, J., and Crossley, M. (1998) *EMBO J.* **17**, 5129–5140
- Palmer, S., Brouillet, J., Kilbey, A., Fulton, R., Walker, M., Crossley, M., and Bartholomew, C. (2001) *J. Biol. Chem.* **276**, 25834–25840
- Gossen, M., and Bujard, H. (1992) *Proc. Natl. Acad. Sci. U. S. A.* **89**, 5547–5551
- Shockett, P., Difilippantonio, M., Hellman, N., and Schatz, D. (1995) *Proc. Natl. Acad. Sci. U. S. A.* **92**, 6522–6526
- Mizushima, S., and Nagata, S. (1990) *Nucleic Acids Res.* **18**, 5322
- Chodosh, L. A., Carthew, R. W., and Sharp, P. A. (1986) *Mol. Cell. Biol.* **6**, 4723–4733
- Morgenstern, J., and Land, H. (1990) *Nucleic Acids Res.* **18**, 3587–3596
- Hochuli, E. (1990) in *Genetic Engineering, Principles and Methods* (Setlow, J., ed) Vol. 12, pp. 87–98, Plenum Publishing Corp., New York
- Grozinger, C., Hassig, C., and Schreiber, S. (1999) *Proc. Natl. Acad. Sci. U. S. A.* **96**, 4868–4873
- Chomczynski, P., and Sacchi, N. (1987) *Anal. Biochem.* **162**, 156–159
- Wells, J., Boyd, K., Fry, C., Bartley, S., and Farnham, P. (2000) *Mol. Cell. Biol.* **20**, 5797–5807
- Pavletich, N., and Pabo, C. (1991) *Science* **252**, 809–817
- Klevit, R. E. (1991) *Science* **253**, 1367, 1393
- Riggs, A., Suzuki, A., and Bourgeois, S. (1970) *J. Mol. Biol.* **48**, 67–84
- Fernandez, P., Frank, S., Wang, L., Schroeder, M., Liu, S., Greene, J., Cocito, A., and Amati, B. (2003) *Genes Dev.* **17**, 1115–1129
- Khanna-Gupta, A., Lopingco, M., Savinelli, T., Zibello, T., Berliner, N., and Perkins, A. (1996) *Oncogene* **12**, 563–569
- Boyer, P., Colmenares, C., Stavnezer, E., and Hughes, S. (1993) *Oncogene* **8**, 457–466
- Shinagawa, T., Dong, H. D., Xu, M., Maekawa, T., and Ishii, S. (2000) *EMBO J.* **19**, 2280–2291
- Stroschein, S., Wang, W., Zhou, S., Zhou, Q., and Luo, K. (1999) *Science* **286**, 771–774
- Moustakas, A., and Kardassis, D. (1998) *Proc. Natl. Acad. Sci. U. S. A.* **95**, 6733–6738
- Feng, X., Lin, X., and Derynck, R. (2000) *EMBO J.* **19**, 5178–5193
- He, J., Tegen, S., Krawitz, A., Martin, G., and Luo, K. (2003) *J. Biol. Chem.* **278**, 30540–30547
- Kurokawa, M., Mitani, K., Irie, K., Matsuyama, T., Takahashi, T., Chiba, S., Yazaki, Y., Matsumoto, K., and Hirai, H. (1998) *Nature* **394**, 92–96
- Izutsu, K., Kurokawa, M., Imai, Y., Maki, K., Mitani, K., and Hirai, H. (2001) *Blood* **97**, 2815–2822
- Keller, J., Mantel, C., Sing, G., Ellingsworth, L., Ruscetti, S., and Ruscetti, F. (1988) *J. Exp. Med.* **168**, 737–750
- Perkins, A. S., Mercer, J. A., Jenkins, N. A., and Copeland, N. G. (1991) *Development (Camb.)* **111**, 479–487
- Cheng, T., Shen, H., Giokas, D., Gere, J., Tenen, D., and Scadden, D. (1996) *Proc. Natl. Acad. Sci. U. S. A.* **93**, 13158–13163
- Tsai, F.-Y., Keller, G., Kuo, F., Weiss, M., Chen, J., Rosenblatt, M., Alt, F., and Orkin, S. (1994) *Nature* **371**, 221–226
- Phillips, R., Ernst, R., Brunk, B., Ivanova, N., Mahan, M., Deanehan, J., Moore, K., Overton, G., and Lemischka, I. (2000) *Science* **288**, 1635–1637
- Shimamoto, T., Ohyashiki, J., Ohyashiki, K., Kawakubo, K., Kimura, N., Nakazawa, S., and Toyama, K. (1994) *Leukemia (Baltimore)* **8**, 1176–1180
- Kumano, K., Chiba, S., Shimizu, K., Yamagata, T., Hosoya, N., Saito, T., Takahashi, T., Hamada, Y., and Hirai, H. (2001) *Blood* **98**, 3283–3289
- Ikonomi, P., Rivera, C., Riordan, M., Washington, G., Schechter, A., and Noguchi, C. (2000) *Exp. Hematol.* **28**, 1423–1431
- Sitailo, S., Sood, R., Barton, K., and Nucifora, G. (1999) *Leukemia (Baltimore)* **13**, 1639–1645
- Yuasa, H., Oike, Y., Iwama, A., Nishikata, I., Sugiyama, D., Perkins, A., Mucenski, M., Suda, T., and Morishita, K. (2005) *EMBO J.* **24**, 1976–1987
- Ezoe, S., Matsumura, I., Nakata, S., Gale, K., Ishihara, K., Minegishi, N., Machii, T., Kitamura, T., Yamamoto, M., Enver, T., and Kanakura, Y. (2002) *Blood* **100**, 3512–3520